Coherence Preserving Reflecting and Crystal Optics

Tetsuya Ishikawa

SPring-8/RIKEN, Japan

Outline

1. Introduction
2. Coherence Preserving X-Ray Mirrors; Present Status
3. Coherence Propagation in Perfect Crystal Optics
4. Summary

Collaborators

X-Ray Mirror Development

Kazuto Yamauchi, Kazuya Yamamura, Hidekazu Mimura, Akira Saito, Katuyoshi Endo, Yuzo Mori (Osaka Univ.), Kenji Tamasaku (RIKEN/SPring-8), Makina Yabashi, Alexei Souvorov (JASRI/SPring-8), Mari Shimura, Yukihito Ishizuka (IMCJ)

Diamond Crystal

Kenji Tamasaku, Tomoyasu Ueda (RIKEN/SPring-8), Makina Yabashi (JASRI/SPring-8), Hitoshi Sumiya, Naoto Toda, Shuichi Sato (Sumitomo Electric Industries)

Coherence Propagation in Dynamical Diffraction

Hiroshi Yamazaki (JASRI/SPring-8)

Coherence Preserving X-Ray Mirror

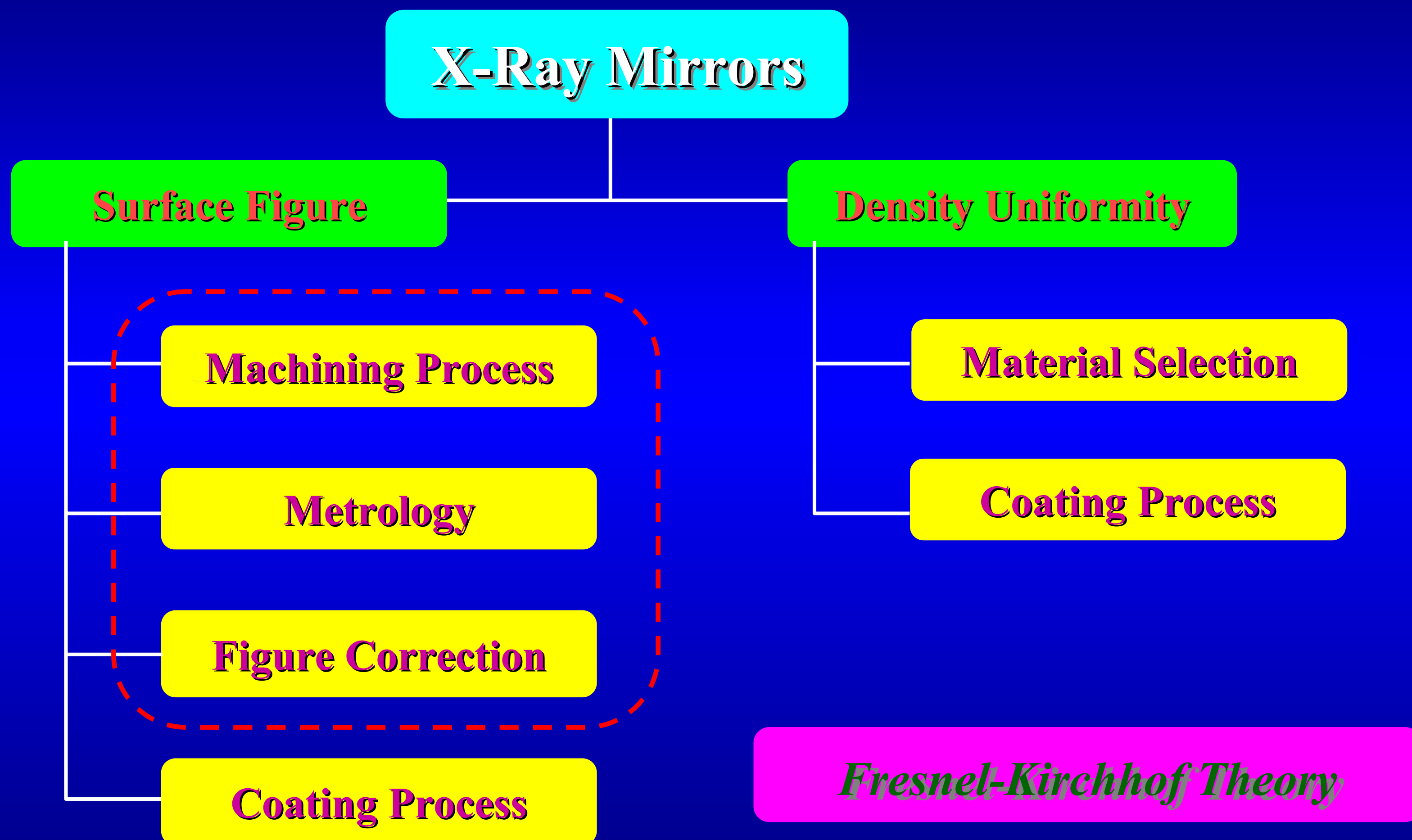

Coherence Preserving Crystal

Crystal

Crystal Perfection

Surface Finish

What we know so far …

Effect of partial coherence on kinematical diffraction
(Sinha et al., PRB, 1998)

Well-prepared Si crystals can preserve x-ray coherence.

Synthetic diamond ?

Dynamical diffraction theory to describe coherence ?

X-Ray Mirrors

Mirror Development & Application

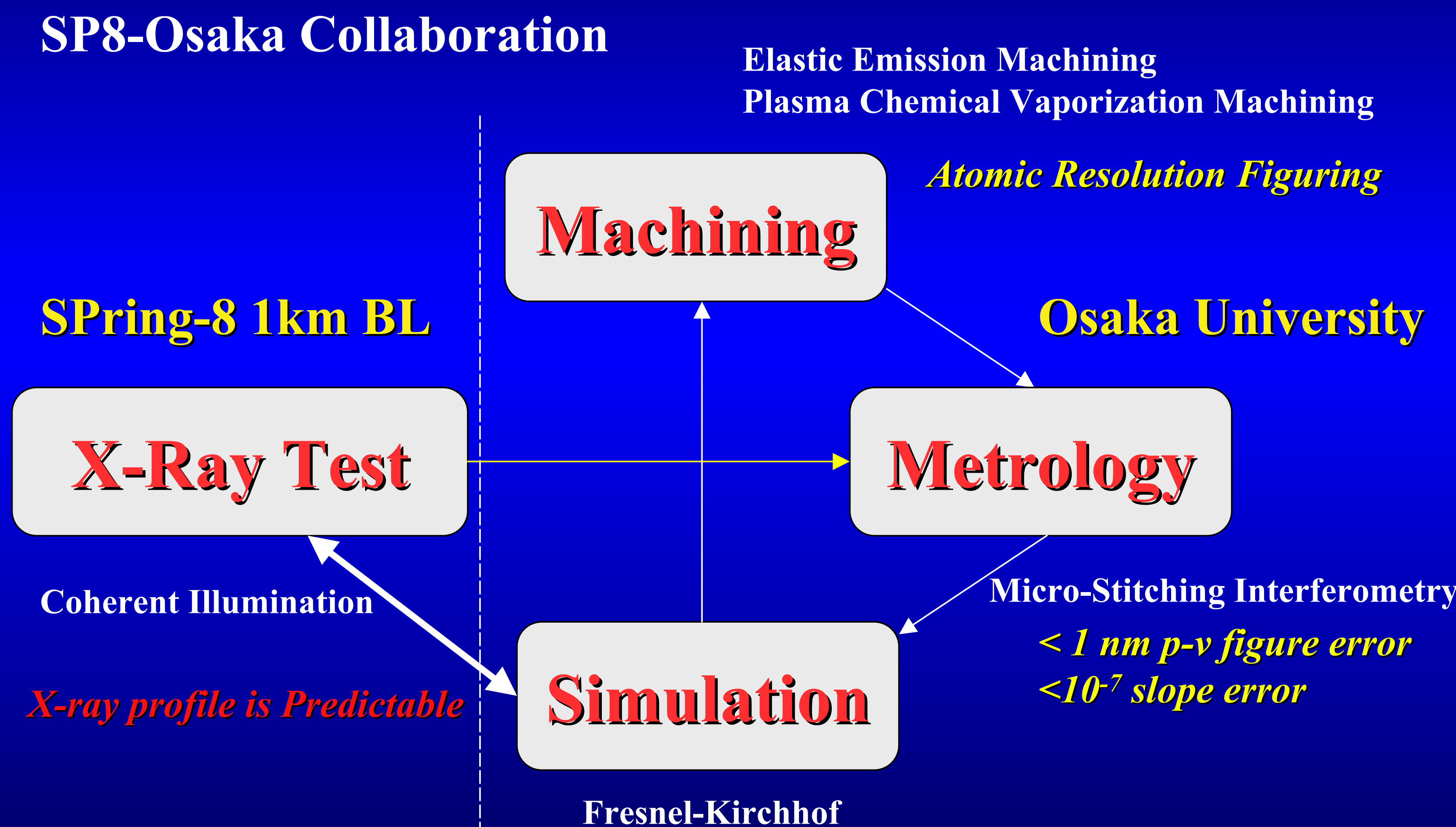

Plasma CVM

1. *A chemical process utilizing reactive species generated in the atmospheric pressure plasma*

↓

Radical density is very high.

High removal rate processing without any crystallographic damage

Material	Removal rate(μm/min)
Fused silica	170
Silicon	94
Molybdenum	36
Tungsten	32
Silicon carbide	6.4
Diamond	2.5

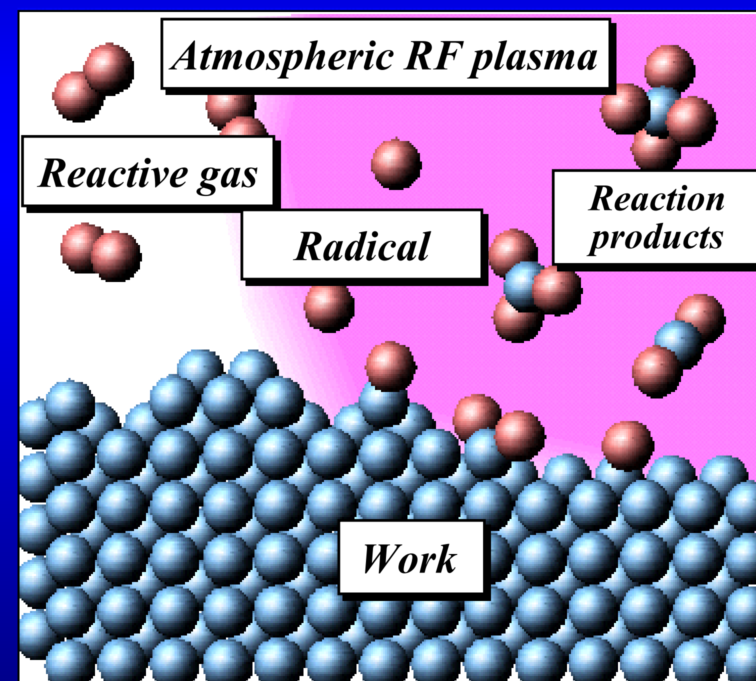

Elastic Emission Machining□□EEM)

An ultraprecision machining process utilizing chemical reaction between surfaces of work and fine powders

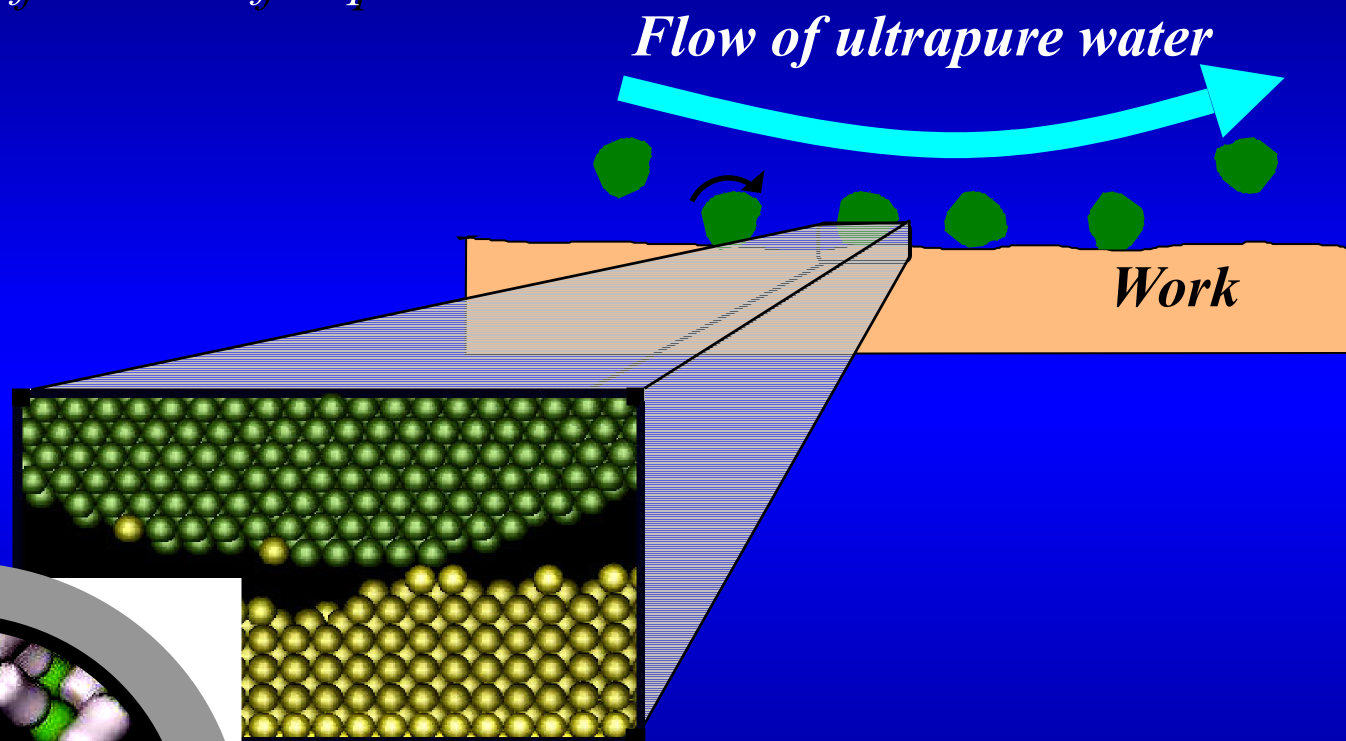

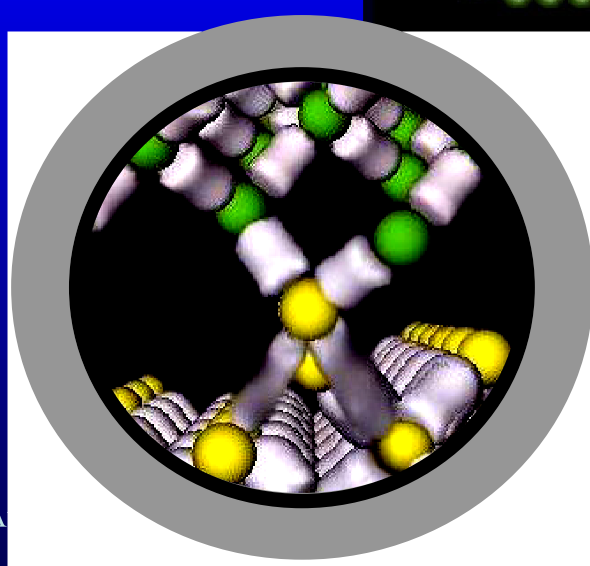

Chemical reactions are induced between only top-site atoms of the work and fine powders

⇩

Automatic smoothing mechanism

A Combined Figure Measurement System

For fabrication process of hard X-ray optics □□□

Figure measurement system with the accuracy of subnanometer-level and with the spatial resolution of submillimeter-level is necessary.

Microscopic interferometer stitching

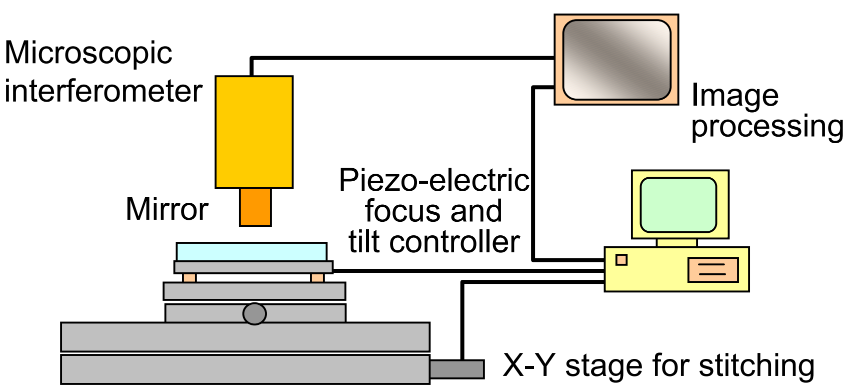

- ***System error is calibrated within 0.1nm(rms)/(5mm×4mm)***
- ***Subnanometer-level accuracy is achievable with the spatial resolution of higher than 0.1mm.***

Large area Fizeau interferometer

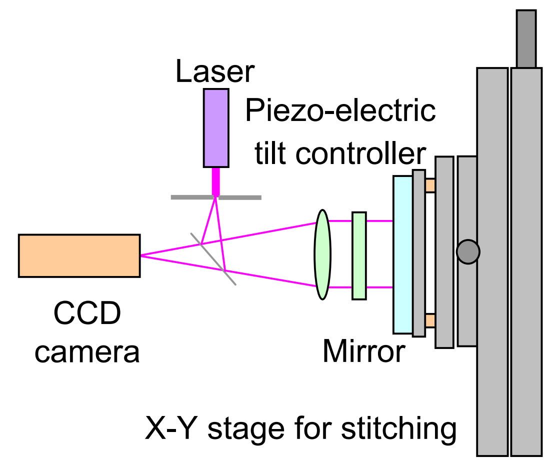

- ***System error is calibrated within 2nm(P-V)/150mm***

Two methods calibrated mutually to the expectable total accuracy higher than 1×10^{-7}rad.

K. Yamauchi et al.
Rev. Sci. Instrum. 74 pp.2894-2898 (2003)

Intensity distribution of reflected X-ray beam

Mori *et al*, *Proc. SPIE* (2001)

Incident angle 1.2mrad / Mirror length 100mm / Mirror material Silicon single crystal (001)

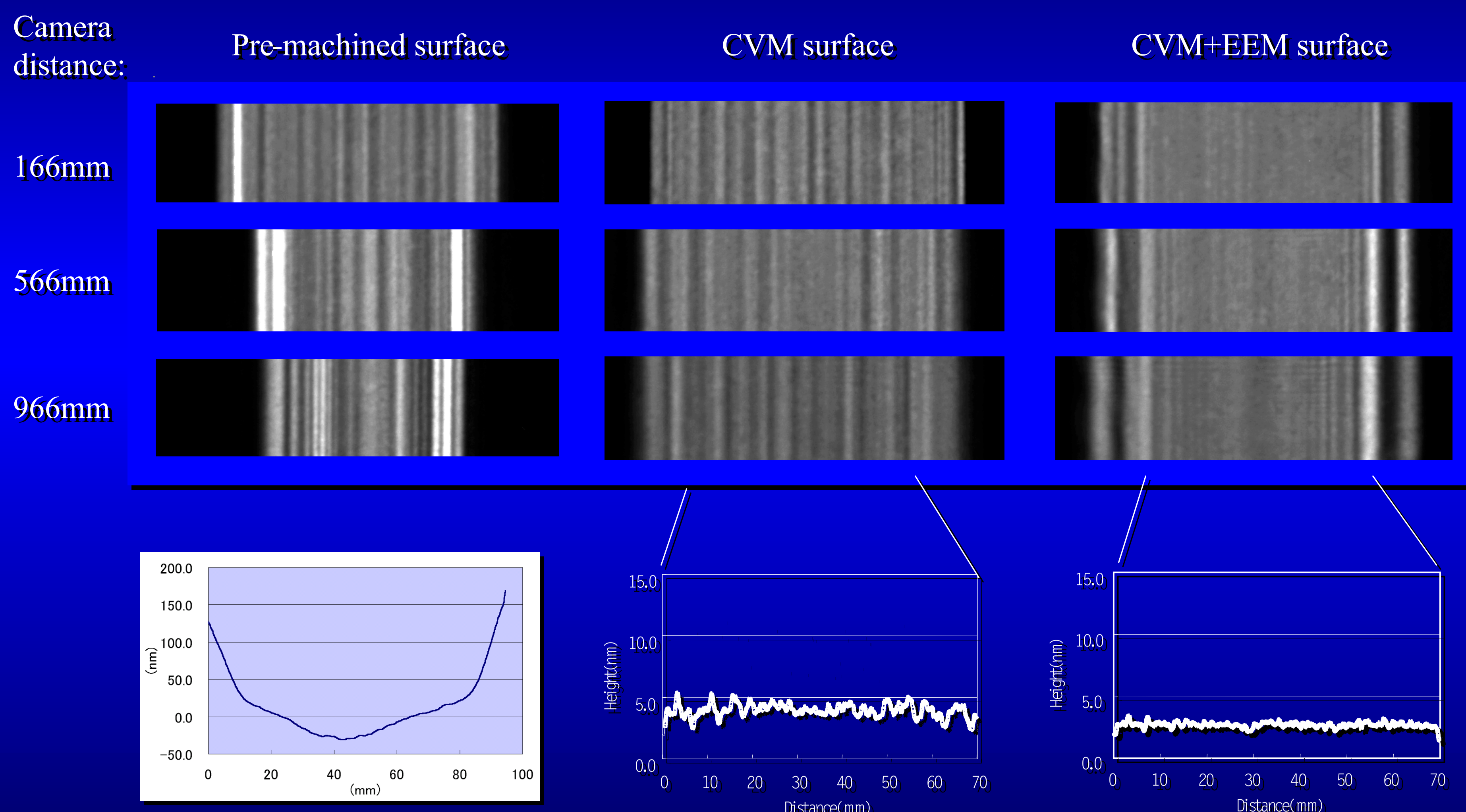

X-Ray Profile ↔ Surface Figure

Wave-Optical Calculation

Yamauchi *et al. submitted to Appl. Opt.*

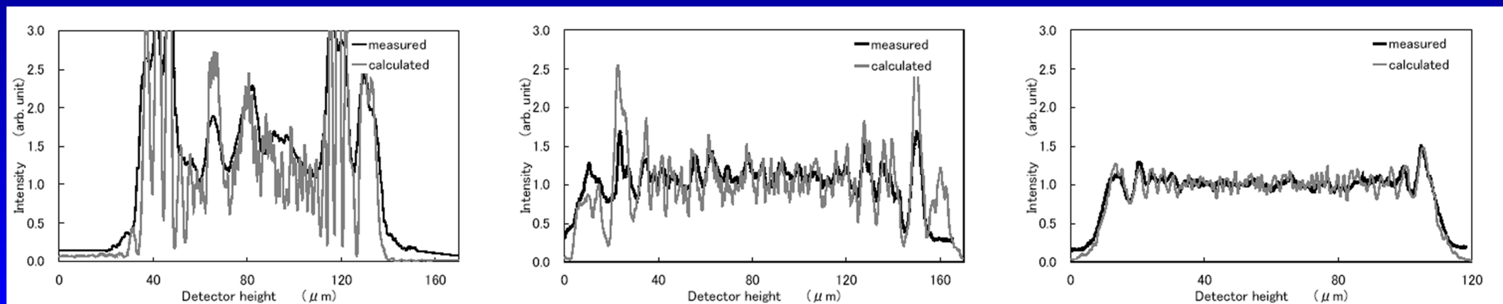

Inverse Problem

Souvorov *et al. J. Synchrotron Rad.* (2002)

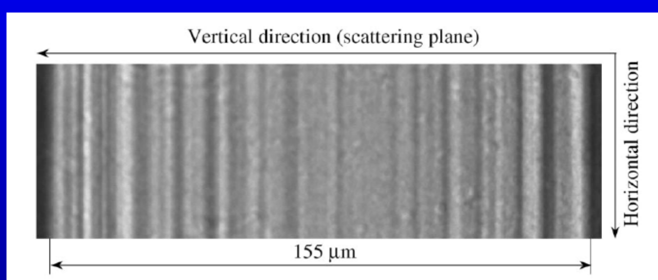

image

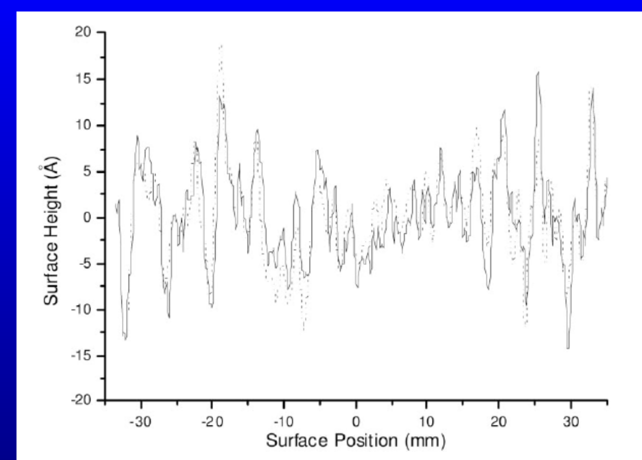

surface profile

Aspherical Mirror Figuring: Elliptical Mirror

Yamauchi *et al.* *JSR (2002)*

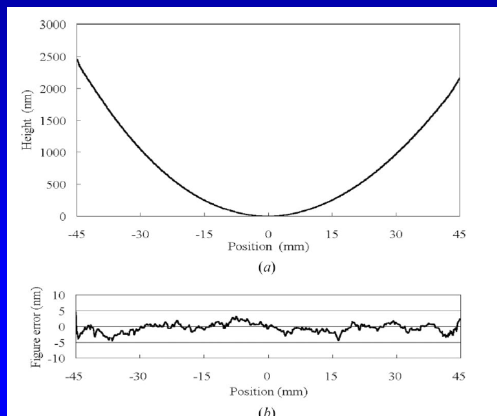

(a) figure and (b) figure error

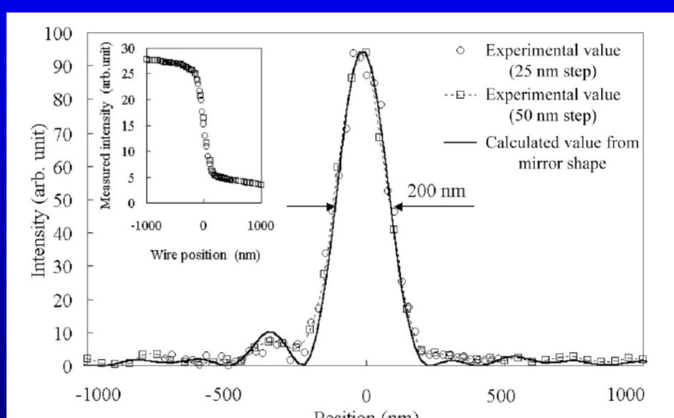

Observed and calculated focal profiles

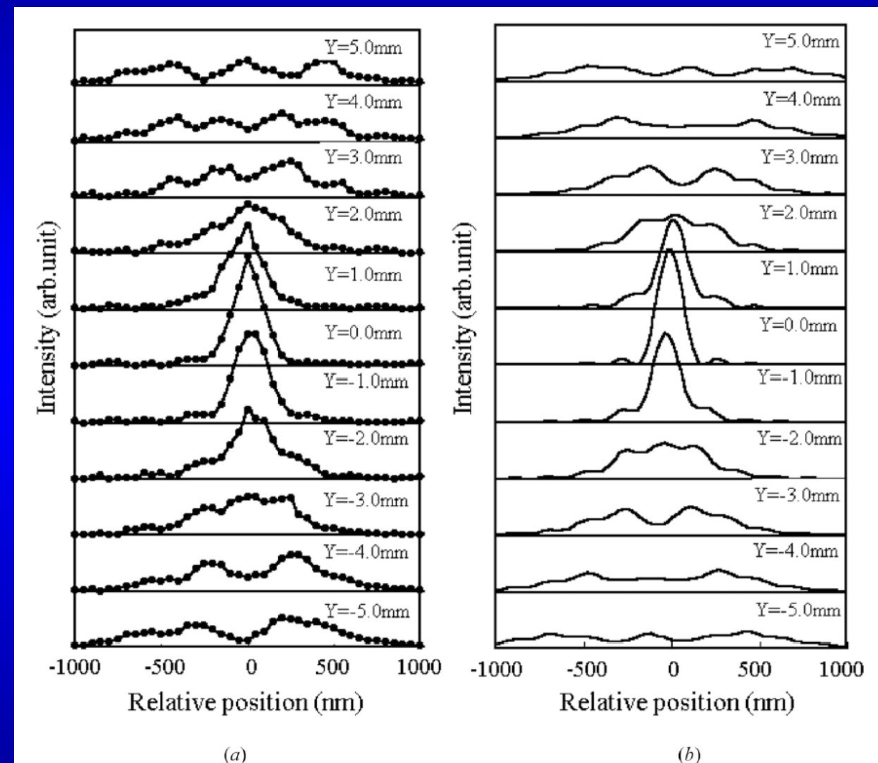

(a) Measured and (b) calculated cross-sectional intensity profiles around the focal spot

Nearly Diffraction-Limited Focusing is Realized !

2D Focusing with KB Configuration

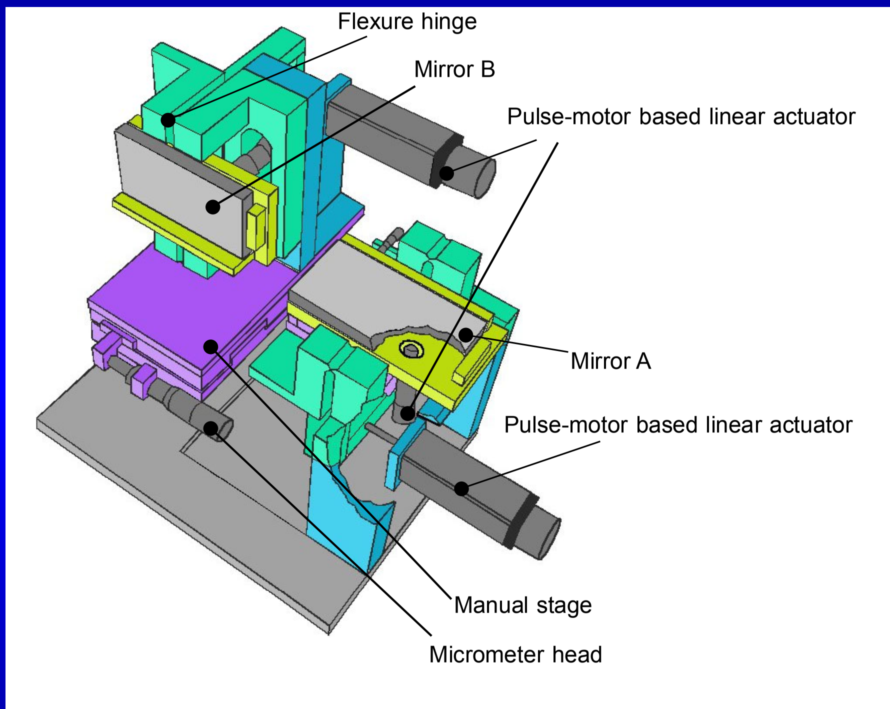

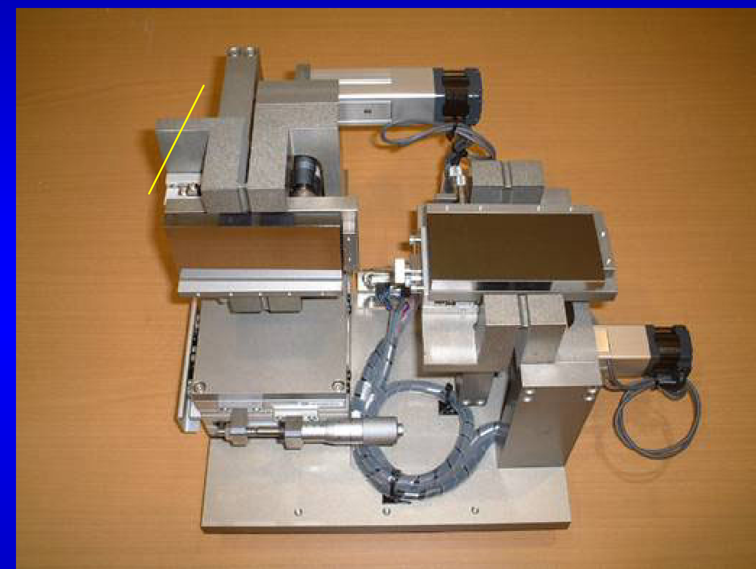

KB mirror aligner

1 hour for alignment
High Stability (>24 hours)

Focusing properties (at the 1 km end-station of SPring-8)

E=15keV(λ=0.8□)

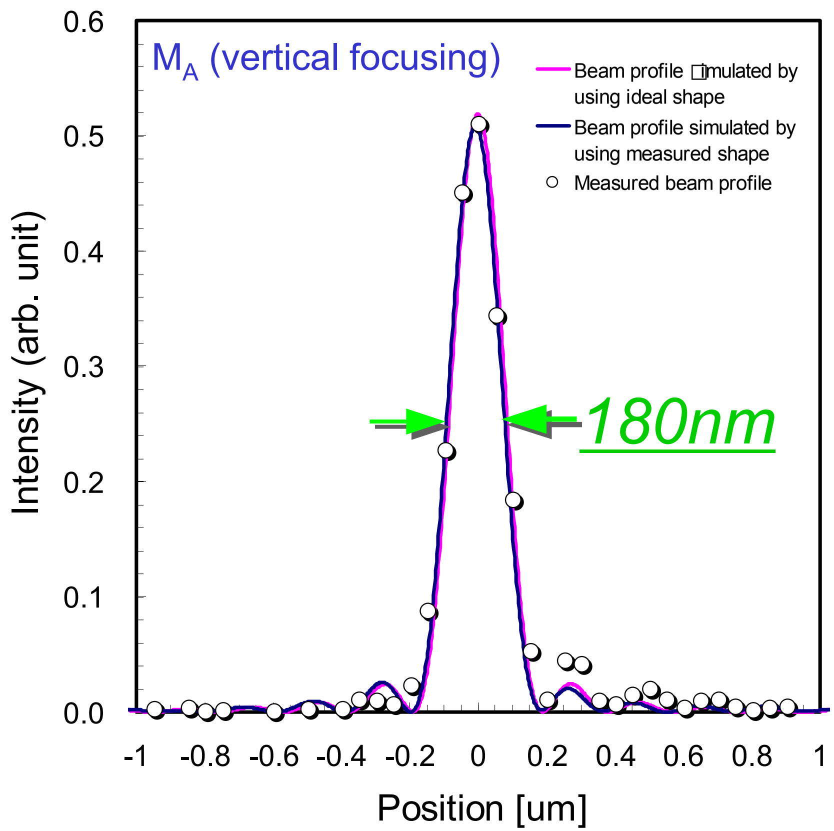

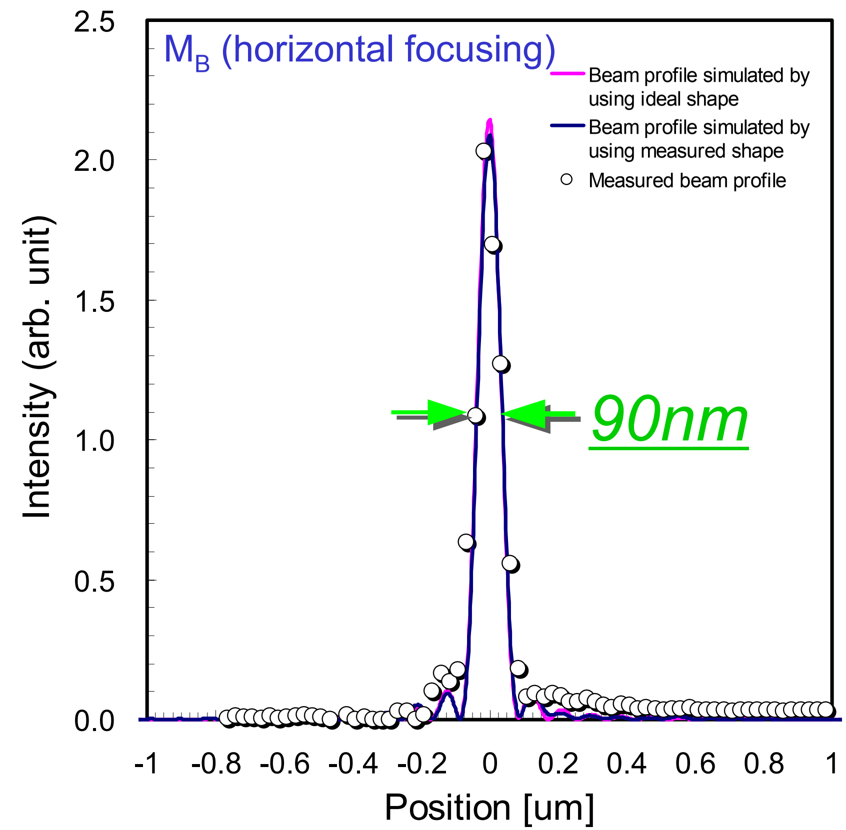

- *Nearly diffraction limited focusing was achieved.*
- *Beam profiles measured and simulated with measured figure agree well.*
  □*Metrology we are using has sufficient accuracy for fabricating X-ray mirrors for coherent illumination.*

Application: X-Ray Fluorescent Microprobe

SP8-Osaka-IMCJ Collaboration

Purpose

Development of Molecular Target Drugs for Cancer

↓

Site-Specific Element Analysis

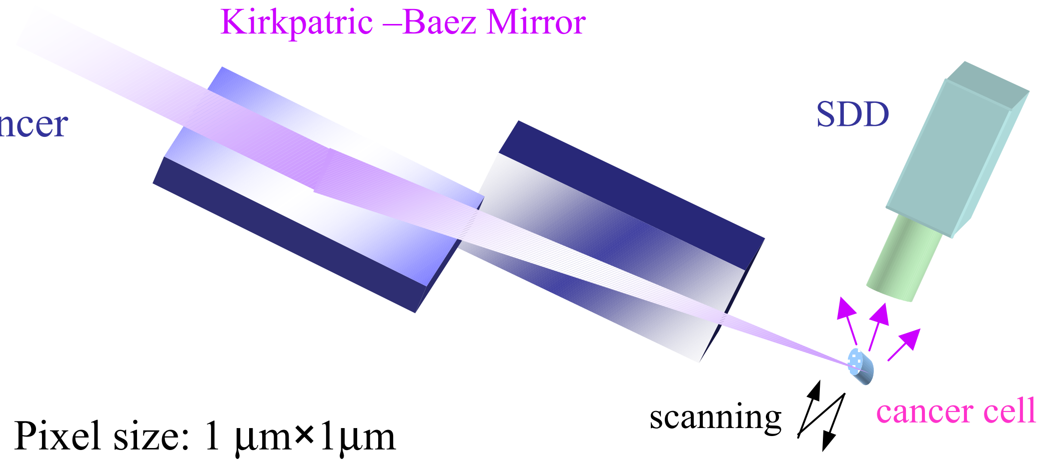

Element Mapping in Cancer Cells

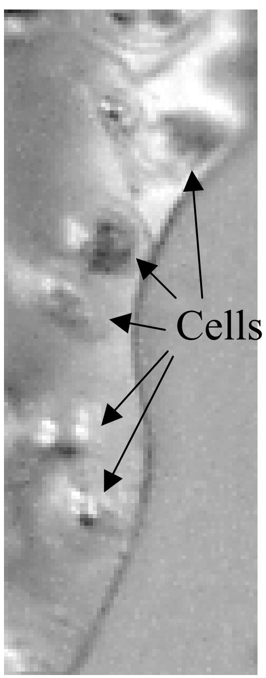

Optical Microscope

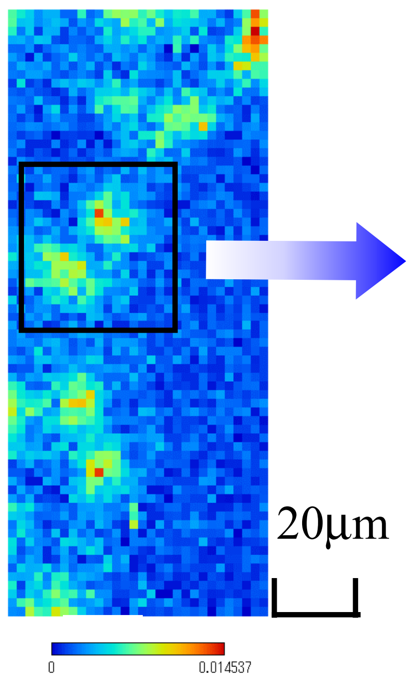

$SK\alpha$ Fluorescence

Pixel size: 1 μm×1μm

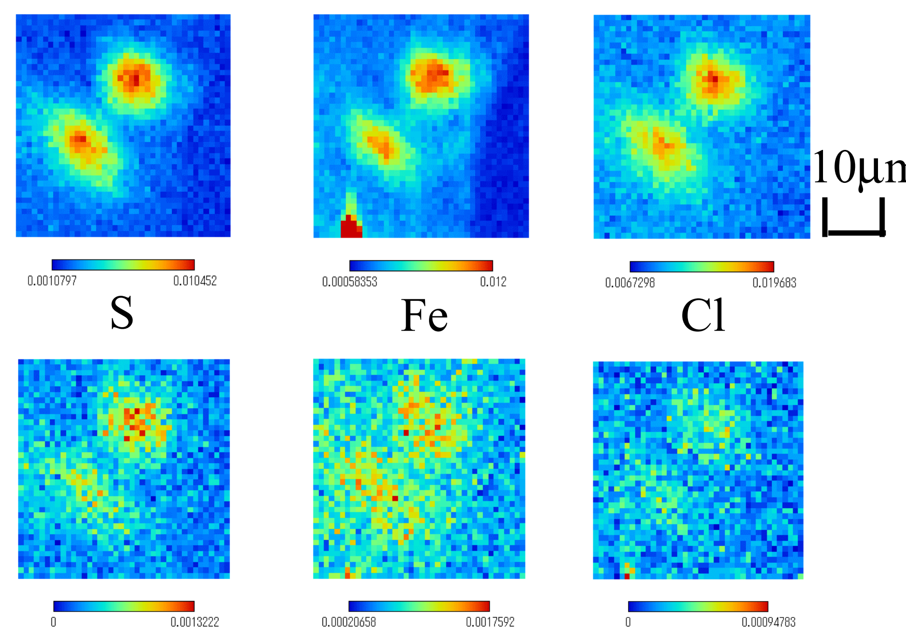

Fluorescence Maps of Several Elements

High Resolution Mapping: 200 nm×200 nm pixel size

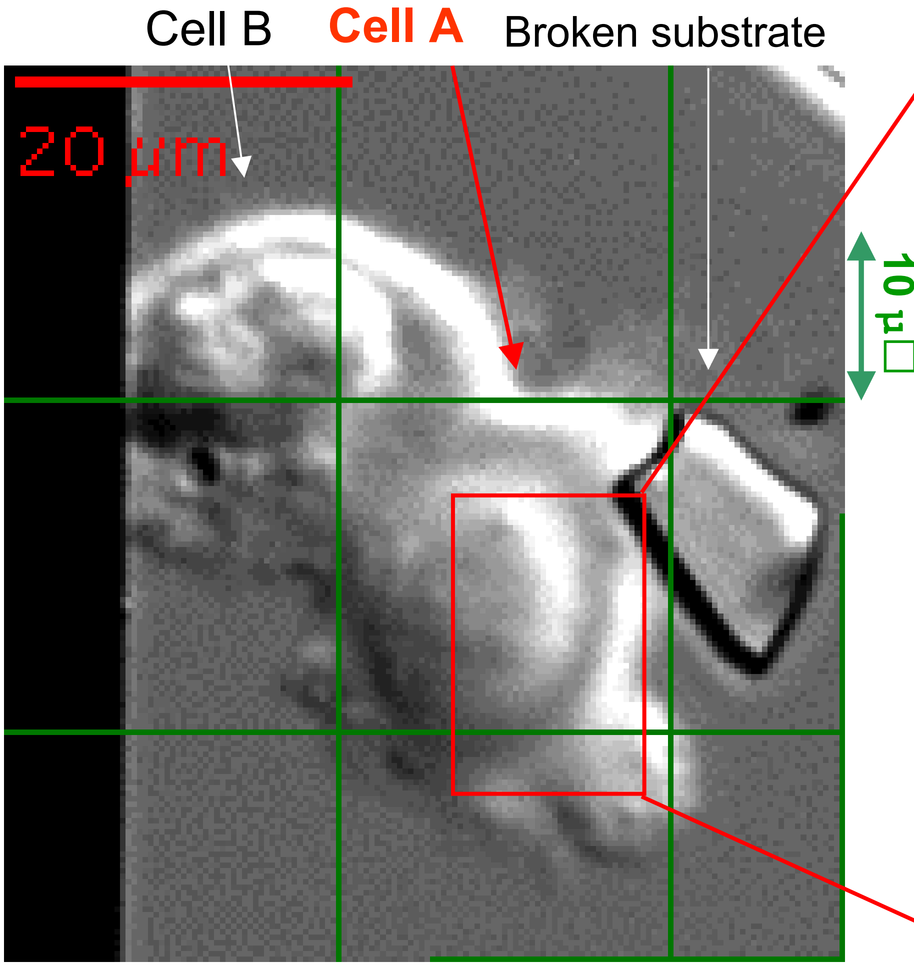

Visible microscope

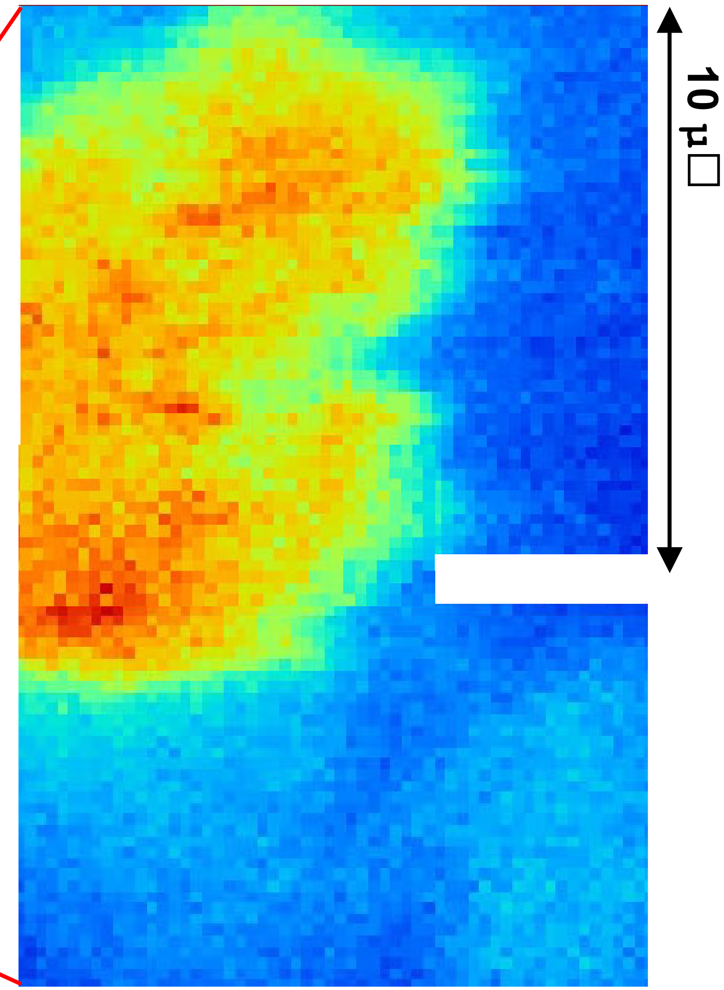

Fe signal (11.1 x 17.3 µ□)

Diamond Crystals

Surface Figure Measurement

(111) Diamond, As-Cleaved Sample

Zygo, New View

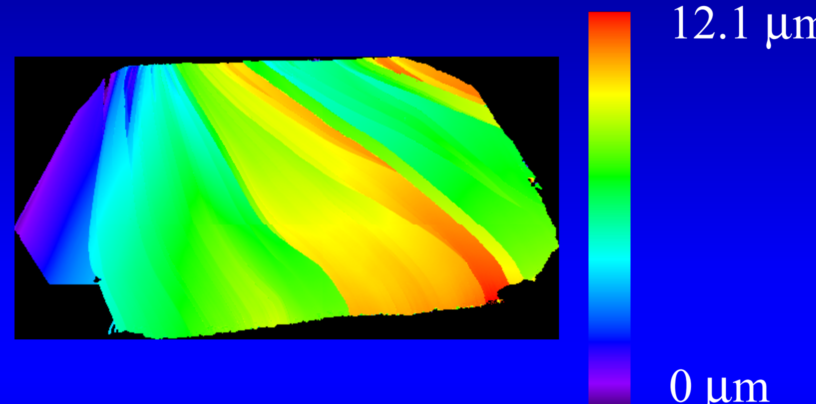

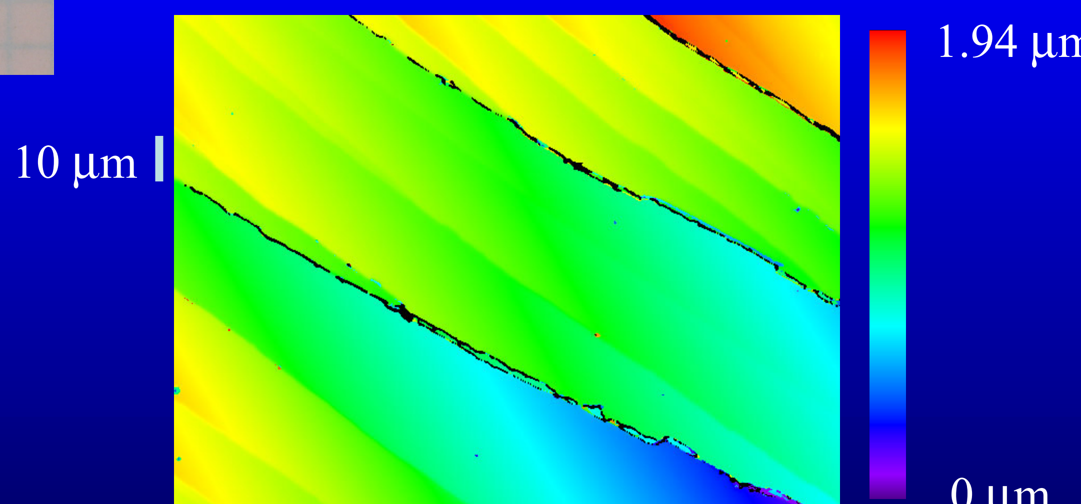

Quasi-Plane-Wave X-Ray Topography

(111) Diamond, As-Cleaved Sample
111 reflection of Diamond, Bragg geometry, E=9.44 keV

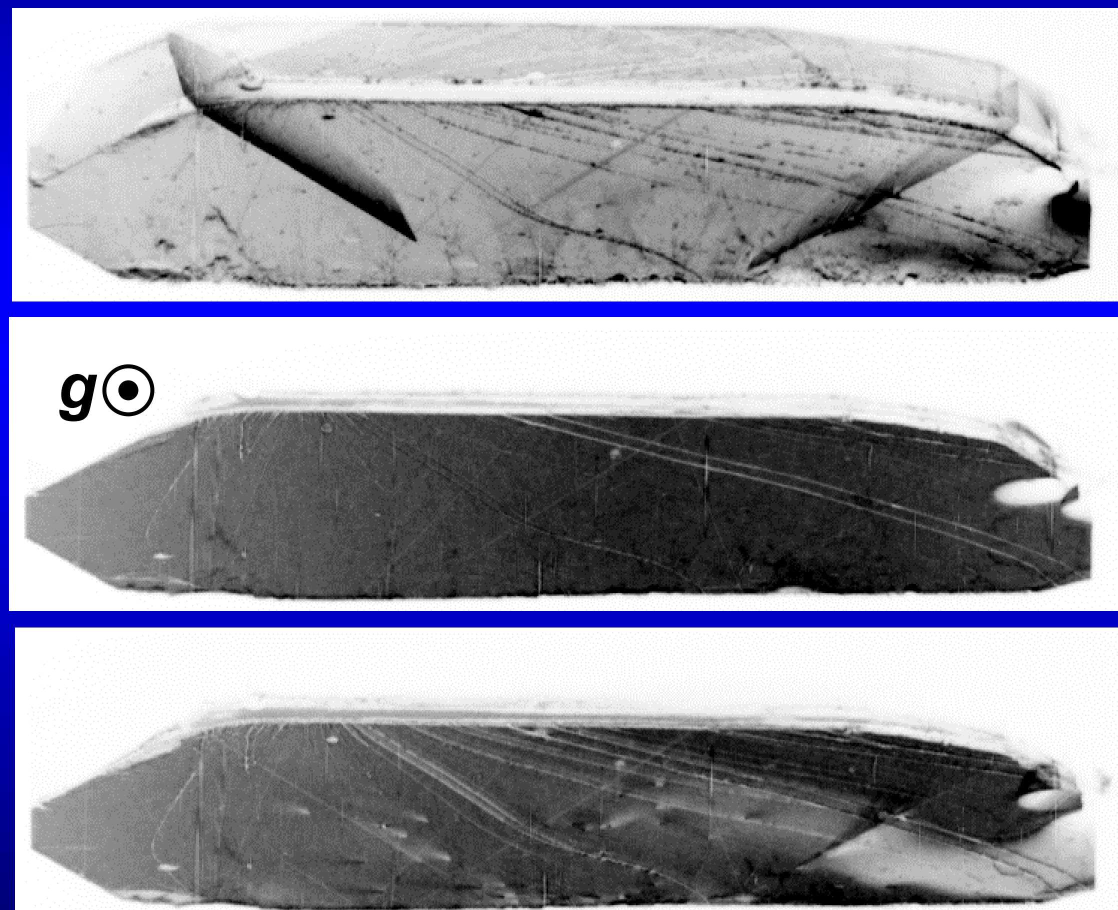

@half max (lower angle)

@center

@half max (higher angle)

Si 220- C 111 Double Crystal

Quasi-Plane-Wave X-Ray Topography

(111) Diamond, As-Cleaved Sample
220 reflection of Diamond, Laue geometry, E=14.55 keV

@half max
(lower angle)

@center

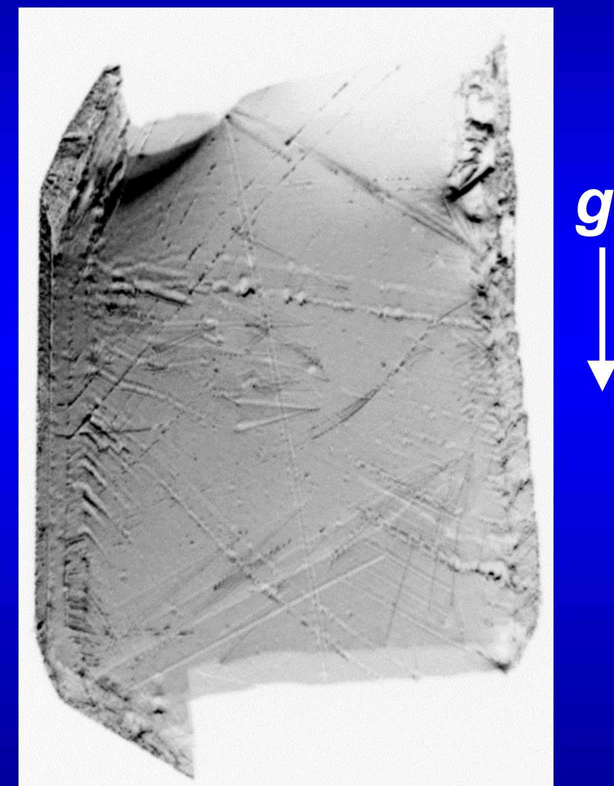

@half max
(higher angle)

Si 331- C 220 Double Crystal

Rocking Curve Measurement

(111) Diamond, As-Cleaved Sample

Bragg Geometry
Si 220(b=20.9)-C 111 @9.44 keV

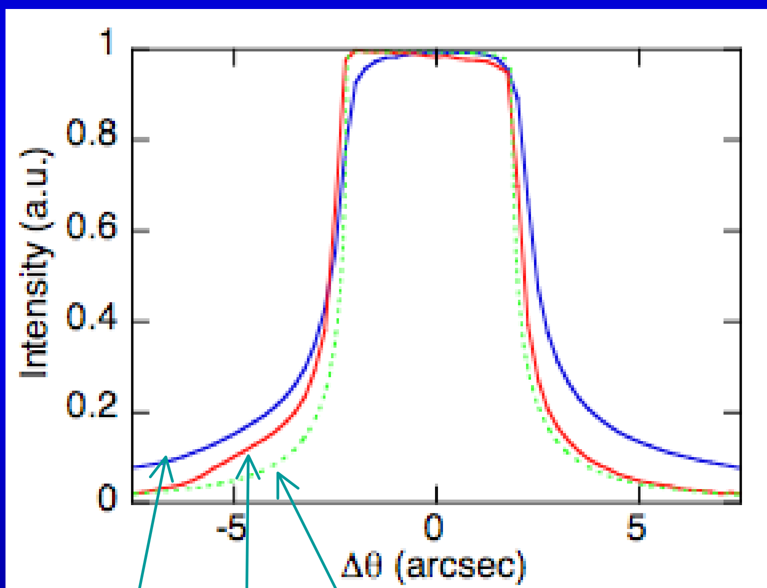

Open Aperture

Intrinsic curve (theory)

Limited Aperture (0.5x0.5 mm^2)

Laue Geometry
Si 331(b=20.9)-C 220 @14.55 keV

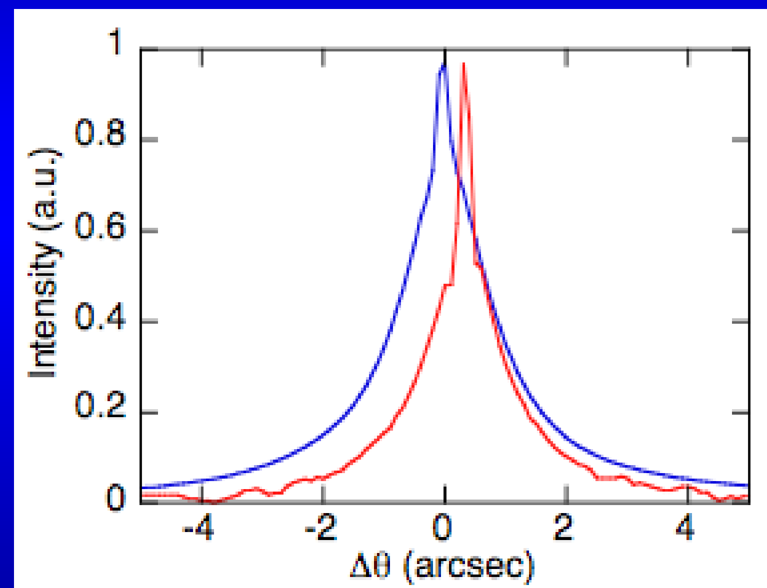

Peak Position/Peak Width Mapping

(111) Diamond, As-Cleaved Sample
111 reflection of Diamond, Bragg geometry, E=9.44 keV
Si 220 (b=20.9)-C 111 Quasi-Parallel Setting

Relative Central Position of Rocking Curves

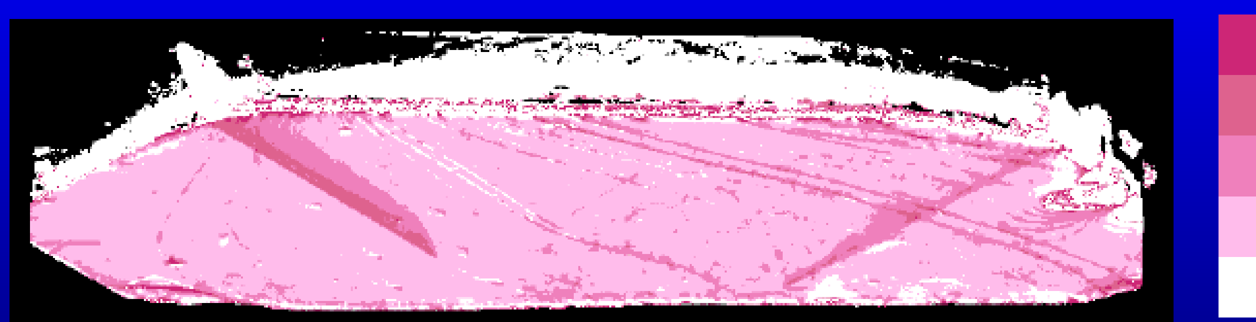

FWHM (Darwin width=4.08”)

Coherence Propagation in Dynamical Diffraction

Coherence Propagation in Dynamical Diffraction

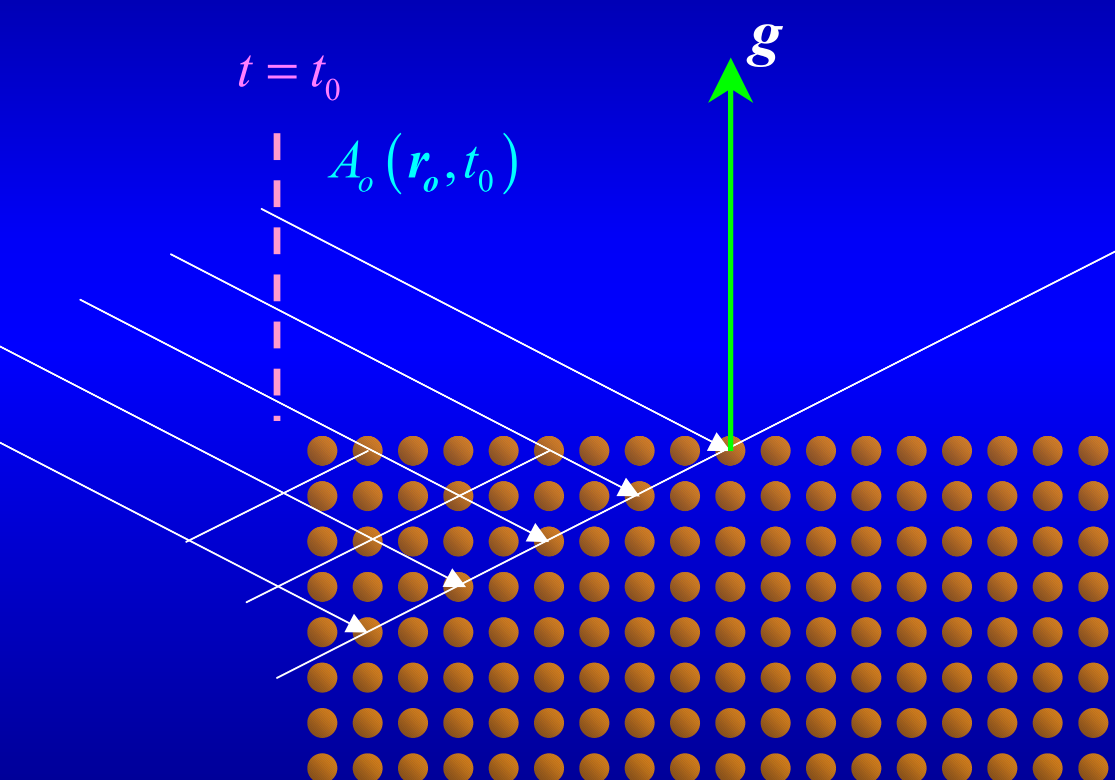

Dynamical diffraction mixes spatial and time coherence.

Coherence preservation in a strict sense for dynamical diffraction is realized only when the incident wavefield is plane-wave.

We cannot separate spatial and time coherence. Mutual coherence function is important.

Coherence Propagation in Dynamical X-Ray Diffraction

Yamazaki & Ishikawa, JAC **35** (2002) 314.

Time-Dependent Takagi-Taupin Equation

$$\left(\frac{\partial}{\partial s_o}+\frac{\partial}{\partial T}-iK\frac{\chi_o}{2}\right)D_o=\frac{iKC\chi_{\bar{h}}}{2}D_h$$

$$\left(\frac{\partial}{\partial s_h}+\frac{\partial}{\partial T}-iK\frac{\chi_o}{2}\right)D_h=\frac{iKC\chi_h}{2}D_o$$

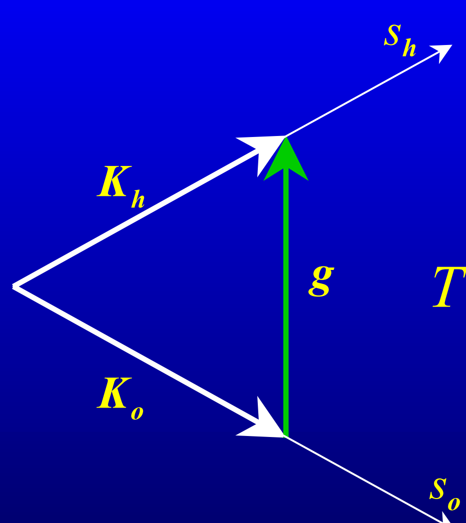

$T = ct$

Wavefields inside the Crystal

$$D_j(Q,T)=\gamma_o\int d\xi_P D_o(P,T-u-v)U_j(P;Q)$$

$U_j(P;Q)$: time-independent propagator

$P(s_o,s_h),\ \ Q(s'_o,s'_h)$

$u=s'_o-s_o, v=s'_h-s_h$

$\gamma_o=\hat{\mathbf{s}}_o\cdot\hat{\boldsymbol{n}},\ \gamma_h=\hat{\mathbf{s}}_h\cdot\hat{\boldsymbol{n}}$

$b=\gamma_o/\gamma_h$;*asymmery factor*

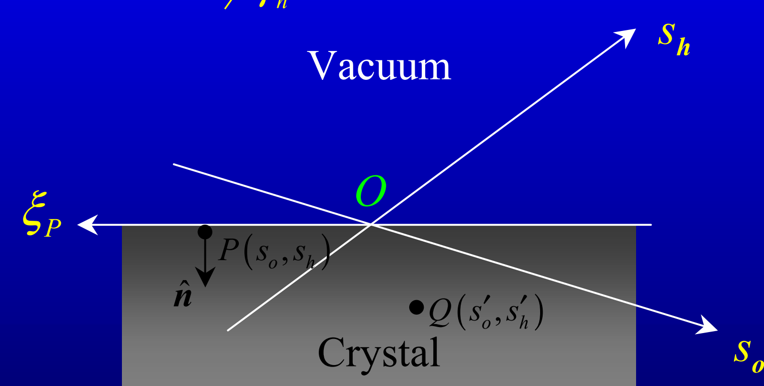

Time-Independent Propagators

Laue Geometry

$$U_o(P;Q)=\frac{1}{\sin 2\theta_B}\left\{\Theta(u)\delta(v)\exp\left(\frac{iK\chi_o u}{2}\right)-\kappa\Theta(u)\Theta(v)\sqrt{\frac{u}{v}}J_1\left(2\kappa\sqrt{uv}\right)\exp\left[\frac{iK\chi_o(u+v)}{2}\right]\right\}$$

$$U_h(P;Q)=\frac{iK\chi_h}{2\sin 2\theta_B}\Theta(u)\Theta(v)\sqrt{\frac{u}{v}}J_0\left(2\kappa\sqrt{uv}\right)\exp\left[\frac{iK\chi_o(u+v)}{2}\right]$$

Bragg Geometry

$$U_o(P;Q)=\frac{1}{\sin 2\theta_B}\left\{\Theta(u)\delta(v)\exp\left(\frac{iK\chi_o u}{2}\right)-\kappa\Theta(u)\Theta(v)\left(\sqrt{\frac{u}{v}}-\frac{1}{|b|}\sqrt{\frac{v}{u}}\right)J_1\left(2\kappa\sqrt{uv}\right)\exp\left[\frac{iK\chi_o(u+v)}{2}\right]\right\}$$

$$U_h(P;Q)=\frac{iK\chi_h}{2\sin 2\theta_B}\Theta(u)\Theta(v)\left[J_0\left(2\kappa\sqrt{uv}\right)+\frac{v}{u|b|}J_2\left(2\kappa\sqrt{uv}\right)\right]\exp\left[\frac{iK\chi_o(u+v)}{2}\right]$$

$\Theta(u): \textit{Heaviside step function except that } \Theta(0)=0$

$\delta(v): \textit{Dirac delta function}$

$b = \textit{asymmetric factor}, \kappa = K|C|\left(\chi_h\chi_{\bar{h}}\right)^{\frac{1}{2}}/2$

Vacuum Waves (Bragg Geometry)

Incident Wavefield in Vacuum

$$D_o(s_o, z_o, T) = A_o(s_o, z_o, T)\exp\{iKz_o(\theta_o - \theta_B)\cos\theta_B\}$$

$A_o(s_o, z_o, T)$; *independent of the glancing angle*, θ_o

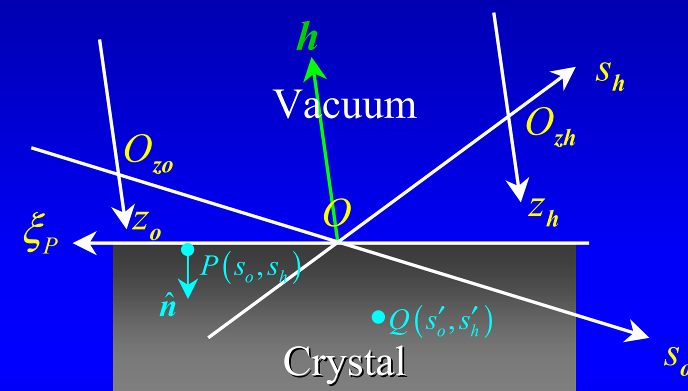

Reflected Wavefield in Vacuum

$$D_h(s_h, z_h, T) = A_h(s_h, z_h, T)\exp\{-iKz_h|b|(\theta_o - \theta_B)\cos\theta_B\}$$

$$A_h(s_h, z_h, T) = \frac{iKC\chi_h}{4\sin\theta_B}\int dz_o A_o(s_o, z_o - |b|z_h, T - s_h + s_o)\exp\left(-\frac{i\kappa z_o W}{\sqrt{|b|}\sin\theta_B}\right)\omega\left(\frac{\kappa z_o}{\sqrt{|b|}\sin\theta_B}\right)$$

$$W = \frac{K}{4\kappa}\sqrt{|b|}\left\{2(\theta_o - \theta_B)\sin 2\theta_B + \chi_o\left(1 - \frac{1}{b}\right)\right\}$$

$$\omega(x) = J_0(x) + J_1(x)$$

Propagation of Coherence Function (Bragg Geometry)

Coherence Function; Goodman 1985

Between two points (s_o, z_{o1}) and (s_o, z_{o2}) on the z_o axis

$$\Gamma_o\left(z_{o1}, z_{o2}; \tau\right) = \left\langle A_o\left(s_o, z_{o1}, T+\tau\right) A_o^*\left(s_o, z_{o2}, T\right)\right\rangle$$

$$\tau; temporal\ delay, \langle \ldots \rangle; time\ average$$

The coherence function on the z_h axis after diffraction

$$\Gamma_h\left(z_{h1}, z_{h2}; \tau\right) = \left\langle A_h\left(s_h, z_{h1}, T+\tau\right) A_o^*\left(s_h, z_{h2}, T\right)\right\rangle$$

$$\propto \int dz_{o1} \int dz_{o2} \Gamma_o\left(z_{o1} - |b| z_{h1}, z_{o2} - |b| z_{h2}; \tau\right) \exp\left\{\frac{i\kappa W\left(z_{o1} - z_{o2}\right)}{\sqrt{|b|}\sin\theta_B}\right\} \omega\left(\frac{\kappa z_{o1}}{\sqrt{|b|}\sin\theta_B}\right) \omega^*\left(\frac{\kappa z_{o2}}{\sqrt{|b|}\sin\theta_B}\right)$$

*Mutual Coherence Function on a line parallel to **h** after diffraction is evaluated from MCF on a line parallel to **h** before diffraction*

Rocking Curve

$$I_h(W) = \left\langle \left| \int_{-\infty}^{+\infty} dz_Q \, A_h(Q,t) \right|^2 \right\rangle$$

$$= \frac{|b||\alpha|^2}{4} \left| \frac{\chi_h}{\chi_{\bar{h}}} \right| \int_{-\infty}^{+\infty} dz_Q \int_{-\infty}^{+\infty} dz_P \int_{-\infty}^{+\infty} dz'_P \Gamma_o(z_P, z'_P)$$

$$\times \exp\left[i\alpha W \left(z_P + |b| z_Q \right) \right] \omega\left[\alpha\left(z_P + |b| z_Q \right) \right] \exp\left[-i\alpha^* W^* \left(z'_P + |b| z_Q \right) \right] \omega^*\left[\alpha\left(z'_P + |b| z_Q \right) \right]$$

$$R(W) = I_h(W) \Big/ \int_{-\infty}^{+\infty} dz_o I_o(z_o) = \int dW' R_i(W') \tilde{g}_o(W - W')$$

$\tilde{g}_o(W - W')$: *Fourier Transform of the Complex Degree of Coherence*

$R_i(W')$: *Intrinsic Profile*

Complex Degree of Coherence

Complex degree of coherence on a line parallel to the reciprocal lattice vector is derived from the measured rocking curve and the calculated intrinsic profile (convolution theorem).

$$g_o(\Delta z_o) = \frac{\int_{-\infty}^{+\infty} d\theta_o R(\theta_o - \theta_B) \exp\left[-iK(\theta_o - \theta_B)\Delta z_o \cos\theta_B\right]}{\int_{-\infty}^{+\infty} d\theta_o R_i(\theta_o - \theta_B) \exp\left[-iK(\theta_o - \theta_B)\Delta z_o \cos\theta_B\right]}$$

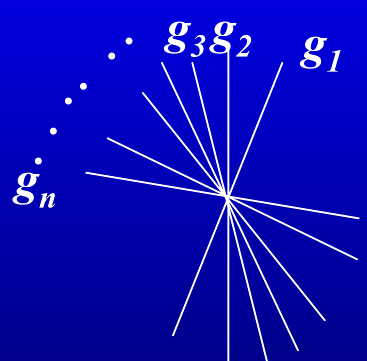

Rocking curves for various **g** will give a spatial distribution of the isochronous complex degree of coherence.

Experimental Determination of Mutual Coherence Function

- Incident Beam: Monochromatic X-Rays from Si 111 or 333 DCM
- (+n, -n, ±m) rocking curve measurements; n = 111, 333; m=111, 333, 444, 555, 777, 888 and 999.
- Derive spatial distribution of isochronous complex degree of coherence.
- Free-Space Propagation to Later Time

Mutual Coherence Function

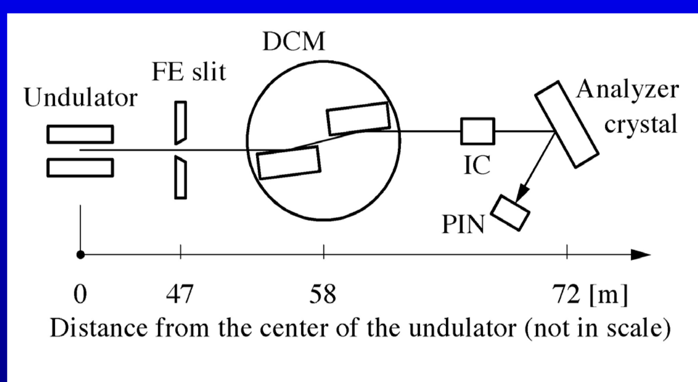

Experimental Setup

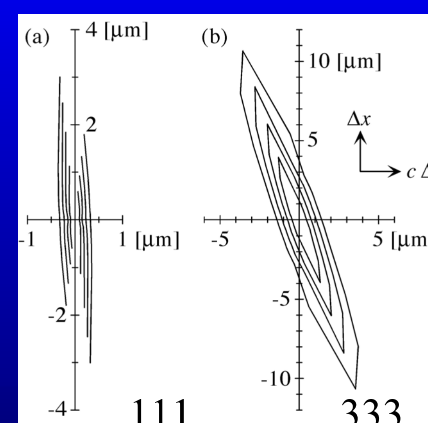

Mutual Coherence Function

Concluding Remarks

- X-ray mirrors preserving coherence is readily available.
- We need to clarify the origin of ‘mosaicity’
- Bragg crystal optics cannot preserve coherence in a strict sense.
- An example to determine the magnitude of mutual coherence function was presented.

Thank you for your attention !

Acknowledgement

X-Ray Mirror Development

Kazuto Yamauchi, Kazuya Yamamura, Hidekazu Mimura, Akira Saito, Katuyoshi Endo, Yuzo Mori (Osaka Univ.), Kenji Tamasaku (RIKEN/SPring-8), Makina Yabashi, Alexei Souvorov (JASRI/SPring-8), Mari Shimura, Yukihito Ishizuka ([illegible])

Diamond Crystal

Kenji Tamasaku, Tomoyasu Ueda [illegible], Makina Yabashi (JASRI/SPring-8), Hiroshi Sumiya, [illegible], Shuichi Sato (Sumitomo Electric Industries)

Coherence Propagation in Dynamical Diffraction

Hiroshi Yamazaki (JASRI/SPring-8)